

Future Change of Storm Surge Risk under Global Warming Based on Mega-Ensemble Global Climate Projections (d4PDF)

Tomoya Shimura¹ and Nobuhito Mori²

Abstract

Long-term assessment of storm surge risk based on the mega-ensemble climate experiment (named as d4PDF), 6000 years historical climate experiment and 5400 years future climate experiment under the assumption of +4K global mean temperature rising, were conducted by super computer in Japan. The d4PDF can provide the statistically-stable estimation of extreme event, 50-100 years return event, for tropical cyclones and storm surges. Future severer storm surges are projected in 15-35N in the Northern Hemisphere. The projected future changes of regional storm surge targeting the Tokyo and Osaka bay in Japan give +0.4 m and +0.2 m increases of 50 year return value of storm surge deviation in comparison with the present climate condition.

Key words: storm surge, climate change, climate projection, extreme value, d4PDF

1. Introduction

Influence of climate change is getting apparent these days. The latest report of IPCC (IPCC-AR5, 2013) states that global mean sea level rose by 0.19 m over the period 1901 to 2010. Climate change can also change long-term characteristics of tropical cyclones. Emanuel (2005) indicated that, since the mid-1970s, tropical cyclones have become increasingly destructive because of longer storm duration and greater intensity. Moreover, concerns about future increase in the number of intense tropical cyclone and related storm surge risk under global warming, are being potentially increased.

However, long-term assessment of storm surge risk for even historical period is quite difficult because extreme storm surge event occurs extremely low probability in comparison with generation and landfall of tropical cyclone. For practical assessment of storm surge risk at specific bay in Japan, historical worst class/credible typhoon such as Vera in 1959 and Nancy in 1961 are assumed to pass across the bay and the storm surge deviation is estimated using pressure and wind fields by parametric typhoon or dynamic modeling. There are two problems in this approach as following: 1) The return period cannot be estimated, 2) The validity is not clear from meteorological point of view. On the other hand, storm surge risk assessment for a specific bay based on general circulation model (GCM) simulations also has difficulties due to the shortness of integrated period, e.g. 100 years. One of the solutions to this difficulty is statistical approach and the several methods have been proposed (Woodruff et al., 2013; Nakajo et al., 2014). However, the uncertainty which arises from lack of observed data for developing statistical model, is increased eventually focusing on limited target area,

Furthermore, projection of future changes in storm surge risk under global warming is required to estimate quantitatively the uncertainty related with climate projection. The main uncertainty of climate projection arises from below. A) Future emission/concentration of greenhouse effect gas, B) Projection models such as General Circulation Model (GCM), C) Natural internal variability. Uncertainties A) and B) can be estimated some extent using climate projections by a variety of GCM under several future emission/concentration scenarios. However, the number of ensemble of climate simulation is small, $O(10)$, for estimating the uncertainty of natural internal variability and thus the uncertainty of extreme and rare event such as large storm surge cannot be estimated so far.

In this study, extremely long-term, over 5000 years, climate simulations for historical and future

¹Disaster Prevention Research Institute, Kyoto University, Japan. shimura.tomoya.2v@kyoto-u.ac.jp

²Disaster Prevention Research Institute, Kyoto University, Japan. mori@oceanwave.jp

warmer climate were conducted using Atmospheric General Circulation Model (AGCM) in order to assess the tropical cyclone and storm surge risks.

2. Methodology

2.1 Large ensemble climate simulations

Large ensemble climate simulations have been performed using Japan Meteorological Agency/Meteorological Research Institute's 60 km atmospheric general circulation model (MRI-AGCM3.2; Mizuta et al., 2012) for global domain and Japan Meteorological Agency/Meteorological Research Institute's 20 km regional climate model (NHRCM; Murata et al., 2013) for around Japan domain downscaled from global domain. This data set is named as "Database for Policy Decision-Making for Future Climate Change (d4PDF)". The d4PDF consists of three experiments under different climate conditions as follows,

- Historical climate experiment
 - Duration: 60 years (1951 – 2010)
 - Ensemble members: 100
 - Total duration: $60 \times 100 = 6000$ years
- 4K temperature increased future climate experiment
 - Duration: 60 years
 - Ensemble members: 90
 - Total duration: $60 \times 90 = 5400$ years

The sea surface temperature (SST) and sea ice condition are the boundary condition, and greenhouse gas concentration is external forcing for MRI-AGCM climate simulations. In the historical climate experiment, period is 1951 to 2010 (60 years) and the observed monthly mean SST and sea ice (Hiraishi et al., 2014) were used for boundary conditions and observed greenhouse gas concentration were used for external forcing. 100 ensemble members were produced by different initial conditions and small perturbations of SST. Therefore, total $60 \times 100 = 6000$ years' results can be available.

In 4K increased future climate, global-mean surface air temperature is assumed to be increased by 4K compared with pre-industrial climate. This assumption is based on GCM climate projections under the Representative Concentration Pathway 8.5 (RCP8.5) scenario in the Coupled Model Inter-comparison Project phase 5 (CMIP5; Taylor et al., 2102) and the projection indicated global-mean surface air temperature would be increased by 4K at the end of 21st century (IPCC-AR5, 2013). The future SST conditions were produced by adding the SST warming patterns to de-trend observed SST during 1951 to 2010. Six SST warming patterns were derived from six CMIP5's GCM climate projections (CCSM4, GFDL-CM3, HadGEM2-AO, MIROC5, MPI-ESM-MR and MRI-CGCM3). The six CMIP5's GCM were selected based on cluster analysis for SST warming pattern (Mizuta et al., 2014); the variation in SST warming pattern by six models can reasonably represent that by 28 models in CMIP5. The greenhouse gas concentration of 2090 level of RCP8.5 scenario was used for external forcing. 15 ensemble members for each SST warming pattern were produced by different initial conditions. Therefore, total $60 \times 6 \times 15 = 5400$ years' results can be available.

GCM climate simulations were downscaled to the East Asia area covering Japan using 20km resolution NHRCM. But, we focused on only GCM results in this study. The detail description of d4PDF can be seen in Mizuta et al. (2017).

The understanding of extreme event level with $O(10) \sim O(100)$ years return period is required for storm surge risk assessment. In this study, the value of R years return period (V_R) is calculated directly from the order statistics not using parametric representation as

$$V_R = (1 - w)x_k + wx_{k+1} \quad (1)$$

where x_k is k th largest value in the annual maximum values and w is the weight factor for interpolation. The value of k is

$$k = \text{floor}(N/R) \quad (2)$$

where N is the number of year and $\text{floor}()$ is the floor function. The value of w is

$$w = N/R - \text{floor}(N/R) \quad (3)$$

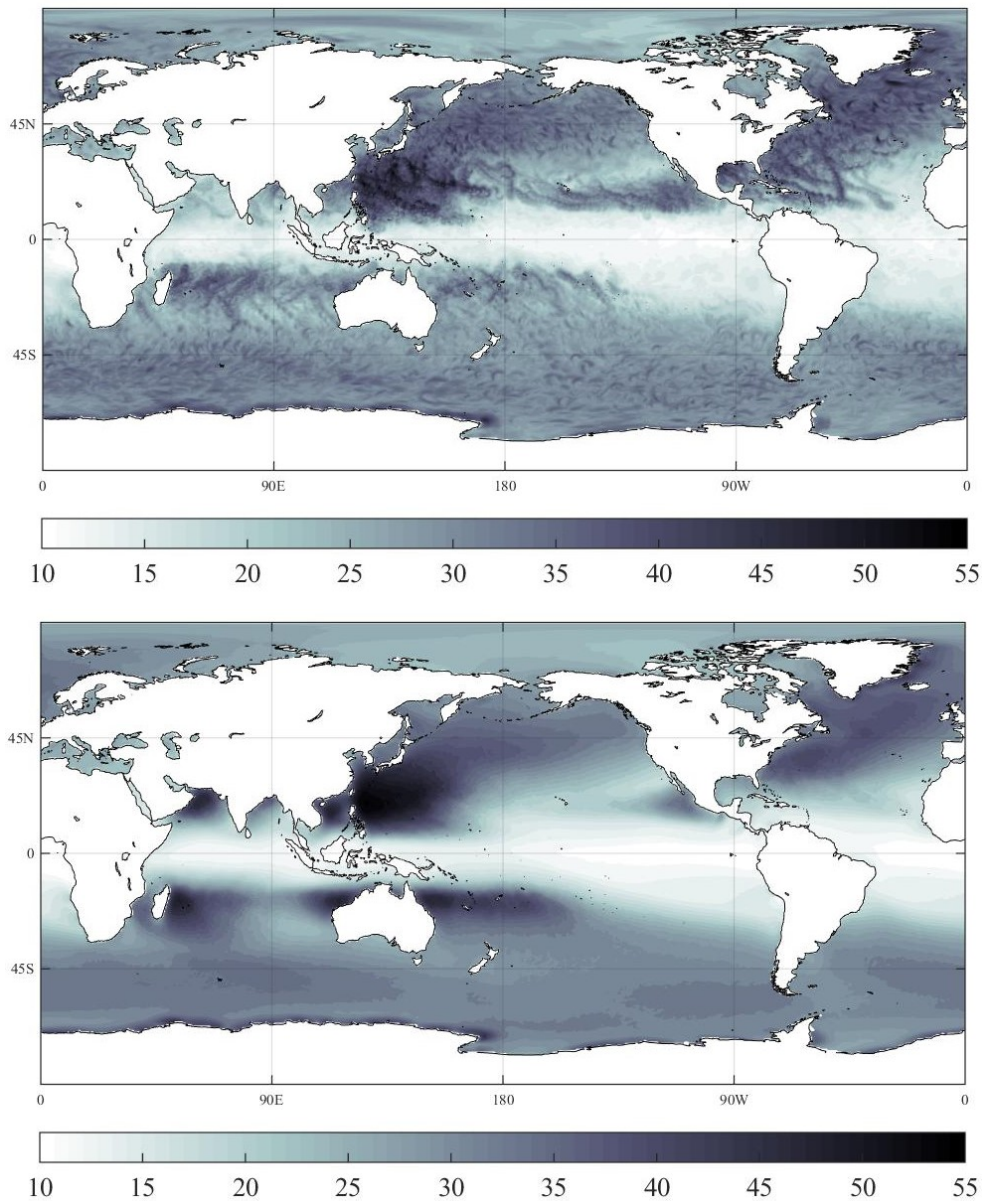


Figure 1. 50 years return value of U_{10} (unit: m/s). Upper panel for JRA-55 (55 years data) and lower panel for d4PDF (6000 years data).

Large storm surge deviation is caused by strong sea surface wind and low atmospheric pressure. Figure 1(a) and (b) show the 50 years return value of sea surface wind (U_{10}) which are derived from 55 years reanalysis data set (JRA-55; Kobayashi et al., 2015) and 6000 years data of d4PDF, respectively. Both show

the stronger wind over higher latitudes and tropical cyclone genesis/passing area, especially in the Western North Pacific. However, Figure 1(a) shows spatially-noisy pattern and individual tracks of intense tropical cyclones can be identified. Therefore, the 50 years U_{10} at specific location derived from JRA-55 strongly depends on just a few extreme events. On the other hand, the spatial distribution in Figure 1(b) is spatially smooth and thus the results don't depend on a few extreme events. Therefore, d4PDF can provide a statistically-stable estimation for extreme value such as 50 years return value.

2.2 Storm surge estimation

Storm surge deviation is estimated for specific bays in Japan and global coast. Computational cost of dynamical storm surge model is too high for over 5000 years data. Therefore, statistical approach was adopted. The methods of statistical storm surge estimation for specific bays and global coast are described below.

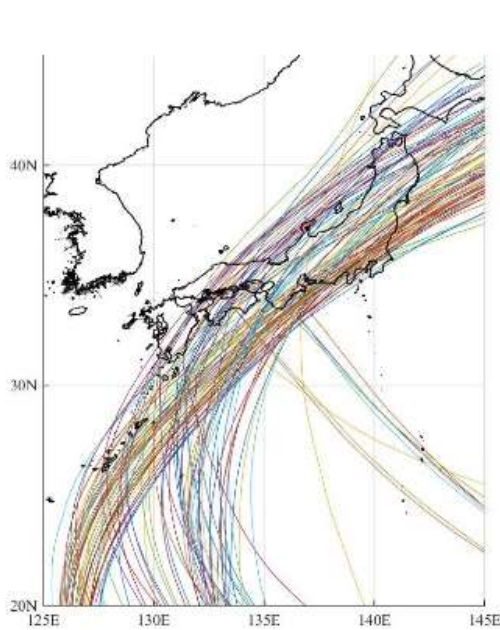


Figure 2. 100 tropical cyclone tracks passing around the Osaka bay

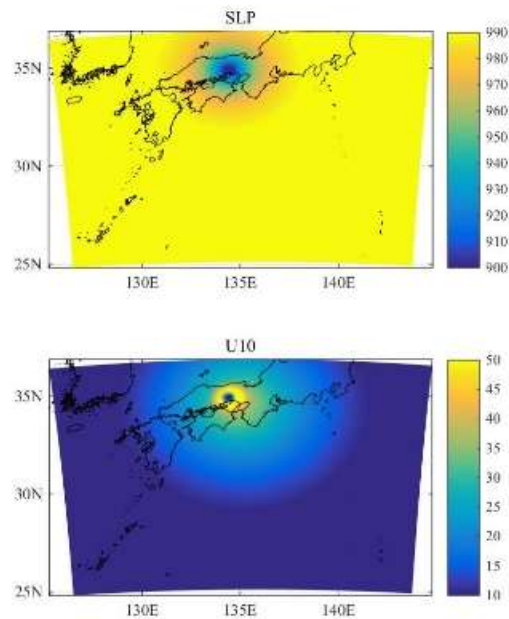


Figure 3. Example of the spatial distribution of SLP (upper panel) and U_{10} (lower panel) for particular TC

2.2.1 Specific bay

Target bays are Osaka and Tokyo bay in Japan. Storm surge deviation (η) is represented as

$$\eta = \eta_p + \eta_w \quad (4)$$

where η_p and η_w are storm surge deviations driven by low pressure and wind. η_p (unit: m) and η_w (unit: m) are represented as

$$\eta_p = 0.01(1010 - SLP) \quad (5)$$

$$\eta_w = AU_{10}^2 \quad (6)$$

where SLP is sea level pressure (unit: hPa) and A is tuning coefficient.

A is determined by storm surge simulations using dynamical model, SuWAT (Kim et al., 2008), which is based on non-linear shallow water equation. 100 tropical cyclones passing the target bay were generated by stochastic tropical cyclone model (Nakajo et al., 2014). The tropical cyclone model can generate various tropical cyclone tracks with various central pressure based on observational characteristics. The 100 tropical cyclone tracks passing around Osaka bay in Japan are shown in Figure 2. The spatial distribution of SLP and U_{10} are determined by parametric typhoon model proposed by Myers and Malkin (1961) and Fujii and Mitsuta (1986), respectively. Figure 3 shows the example of spatial distributions of SLP and U_{10} . 100 storm surge simulations were conducted by SuWAT for the Osaka and Tokyo bay and the tuning coefficient A was determined.

The validity of storm surge estimation by equation (4), (5) and (6) is shown here. Maximum U_{10} at the target location and the SLP at the same time to U_{10} , were used for equation (5) and (6). Maximum storm surge deviations at the target location were estimated for each tropical cyclone. Figure 4 shows the comparison of storm surge deviation at the Osaka bay between statistical (equation (4), (5) and (6)) and dynamical storm surge model. The coefficient A is tuned as 0.0011. The statistical estimation agrees well with dynamical storm surge model results. Therefore, this statistical approach can provide reasonable storm surge estimation.

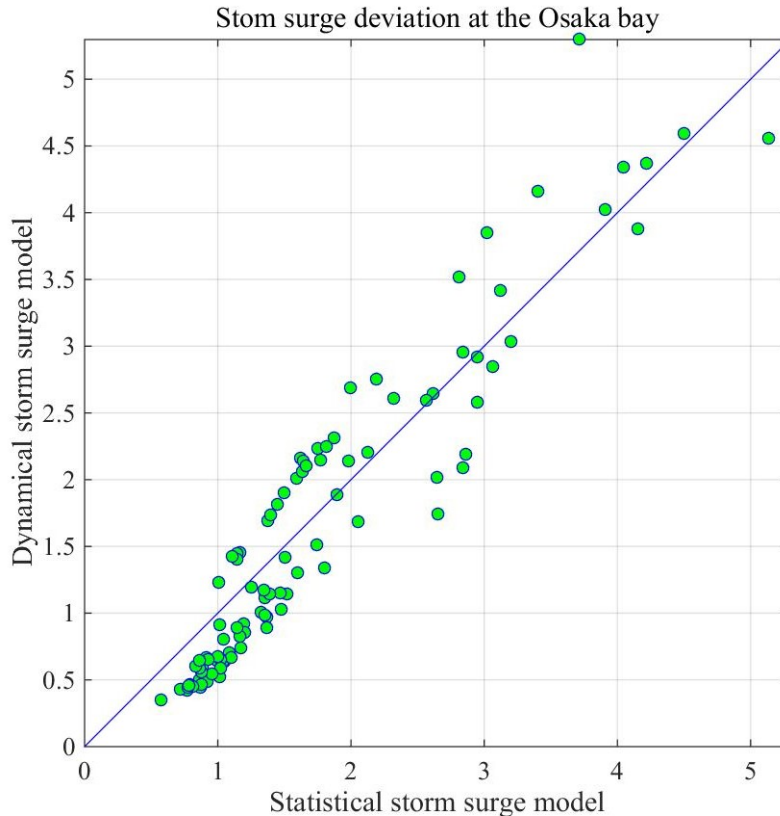


Figure 4. Comparison of maximum storm surge deviation at the Osaka bay between statistical and dynamical storm surge model (unit: m).

2.2.2 Global coast

It is difficult to determine the tuning coefficient A for global coast as section 2.2.1 due to computational cost. Therefore, A is simply determined depending on water depth. A at the Osaka bay is set

to reference value and the A is represented as,

$$A = A_{osaka}r \quad (7)$$

$$r = d_{osaka}/d \quad (8)$$

where r is depth factor, A_{osaka} is tuning coefficient A at the Osaka bay (0.0011), d is water depth averaged 50 km around target coast and d_{osaka} is water depth at the Osaka bay (25m). Maximum value of r is set to 2. This determination of A might be incomplete. Thus, absolute value is not provided in this study and projected future change ratio in storm surge is estimated. If η_w is much larger than η_p , projected future change ratio depends just on U_{10}^2 change but A .

3. Projected future change of tropical cyclone and storm surge

Projected future changes in tropical cyclone, sea surface wind speed and storm surge are described in this section. Projected future change is defined as the difference of the value in 4K increased future climate experiment to that in historical climate experiment.

3.1 Tropical cyclone

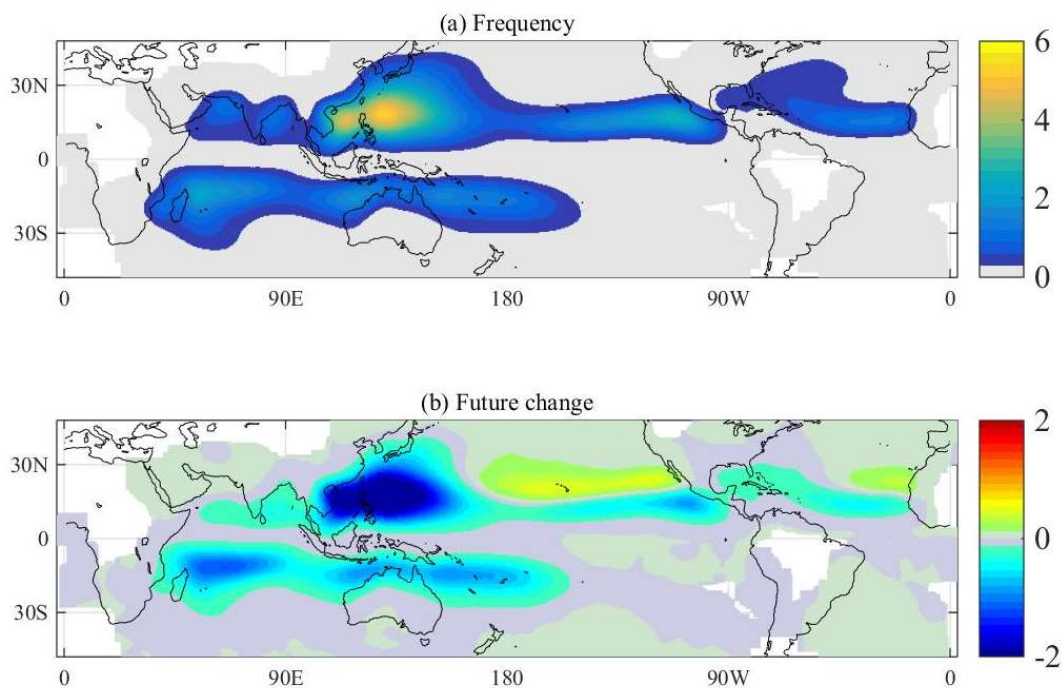


Figure 5. The mean tropical cyclone frequency distribution in the historical experiment (upper panel) and the projected future change (lower panel) (unit: #/year).

Projected future changes in tropical cyclone characteristics directly connects to that in storm surge risk. Tropical cyclones in the climate simulations were detected objectively by the method of Murakami et al. (2014). The tropical cyclone characteristics in the historical climate experiment were compared with observation (IBTrACKS; Knapp et al., 2010). As the result, strong tropical cyclone, such as over 50 m/s maximum wind speed, can be reproduced by d4PDF. And the relationship between central pressure and maximum wind speed by d4PDF agrees with observation.

Figure 5 shows the mean tropical cyclone frequency distribution in the historical experiment and

the projected future change. The tropical cyclone frequency of the Western North Pacific is the highest in the global domain. The projected future changes are characterized by the decreases in frequency over the vast area of global domain, especially in the Western North Pacific, and the increase over the 15N latitudes in the Eastern North Pacific and Eastern North Atlantic.

Projected changes in tropical cyclone intensity is described here. Figure 6 shows the exceedance probability of tropical cyclone's central pressure in global domain and the Western North Pacific. It is clear that stronger tropical cyclones tend to occur over the Western North Pacific. The global annual mean tropical cyclone numbers in the historical and future climate experiment are 85 and 55 #/year, respectively. In case of the Western North Pacific, annual mean tropical cyclone numbers in the historical and future climate experiment are 30 and 16 #/year, respectively. This decreases in tropical cyclone frequency for both global and the Western North Pacific are due to decreases in relatively less intense tropical cyclone frequency. On the other hand, intense tropical cyclone number is increased. The level of over 1 year return level in the future climate is greater than historical climate. The 100 years return level of central pressure would be increased by about 10 hPa.

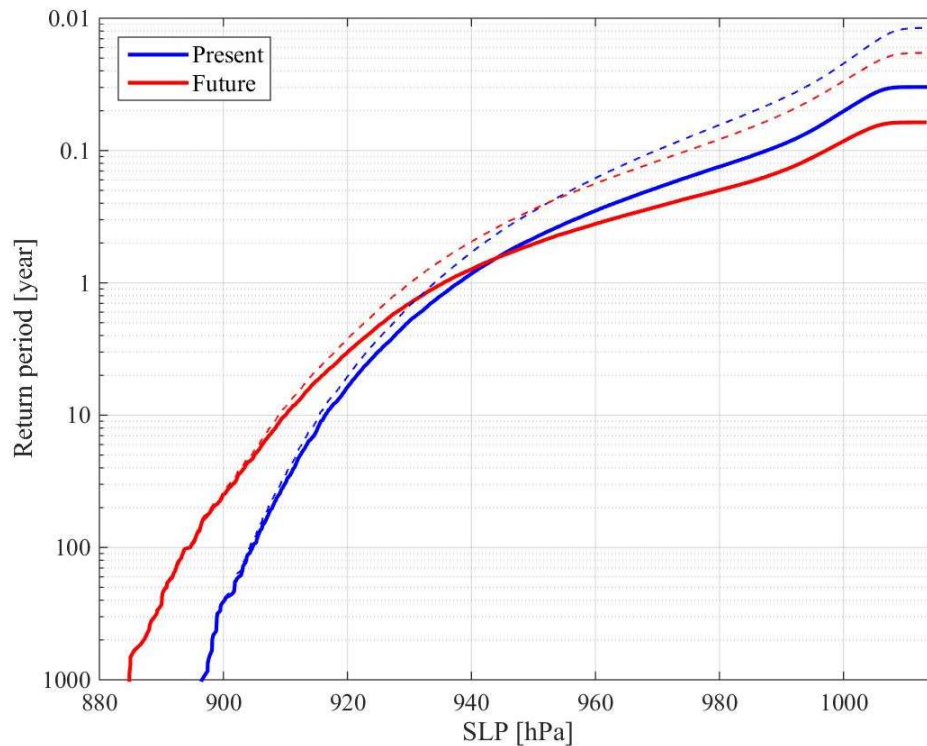


Figure 6. The exceedance probability of tropical cyclone's central pressure in global domain (broken line) and the Western North Pacific (solid line). Blue and red lines mean historical and future climate experiment, respectively.

In addition to frequency and central pressure, the projected changes in track are important tropical cyclone characteristics for impact assessment. Previous studies indicated that tropical cyclone tracks would be shifted north-eastward in the Western North Pacific under warmer future climate (e.g. Mori, 2012). Here, ocean areas are designated as the North Indian Ocean, the Western North Pacific, the Eastern North Pacific, the North Atlantic, the South Indian Ocean, the South Pacific and the South Atlantic, and the centroids of genesis, most development and lysis location were calculated. The projected longitudinal movement of the centroids is greater twice than meridional one. The magnitudes of projected movement of the centroids are as genesis > most development > lysis location except for the North Indian Ocean. The centroids are projected to move towards the center of Ocean longitudinally, eastward in case of the Western North Pacific, and towards the Polar meridionally, northward in the Northern Hemisphere and southward in the Southern

Hemisphere.

3.2 Sea surface wind speed

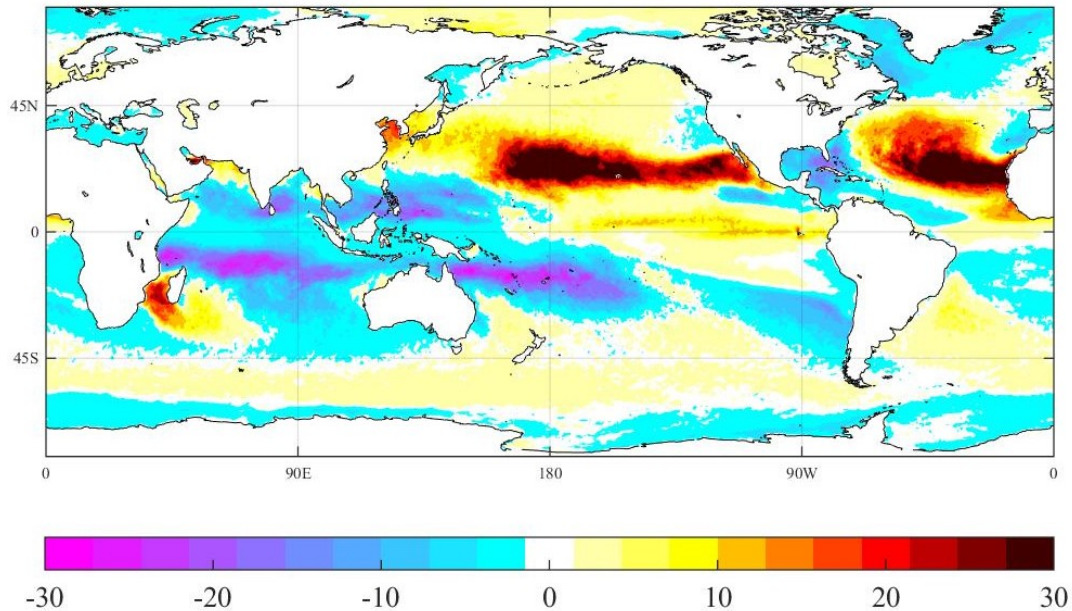


Figure 7. Projected change in 50 year return value of U_{10} (unit: percent)

Figure 7 shows the projected change in 50 year return value of U_{10} . The spatial pattern is characterized as decreases over tropics and increases over extra tropics especially the Eastern North Pacific and Eastern North Atlantic. These projected changes in extreme wind speed correspond to those in tropical cyclone characteristics. The decreases in extreme wind speed in the tropics correspond to decreases in tropical cyclone frequency. The increases in extreme wind speed in the Eastern North Pacific and Eastern North Atlantic correspond to the tropical cyclone track change. The increases in extreme wind speed by 10% in the Western North Pacific are due to the future intensified tropical cyclone.

Figure 8 shows the exceedance probability of U_{10} at the Osaka bay. The variation of extreme wind speed among ensemble members is larger compared with the projected changes in overall ensemble value. For example, in case of 50 years return value, there is over 20 m/s range between ensemble members and the projected change of ensemble mean is about 4 m/s. This variation between ensemble members is due to natural internal variability and irregularity in tropical cyclone characteristics. The variation is larger with longer return period. Therefore, we find that estimation of range of projected changes in extreme value requires large number of ensemble. As overall ensemble value, historical climate value is larger than future below 5 year return period and smaller beyond 5 year return period. Projected future decreases in wind speed of shorter return period are due to decreases in tropical cyclone frequency and the projected increases in extreme wind speed of longer return period are due to future intensified extreme tropical cyclone and track shift. As described above, future changes in extreme wind speed depend on multiple effects of projected changes in regional tropical cyclone characteristics. The tendency at the Tokyo bay is almost same as Figure 8.

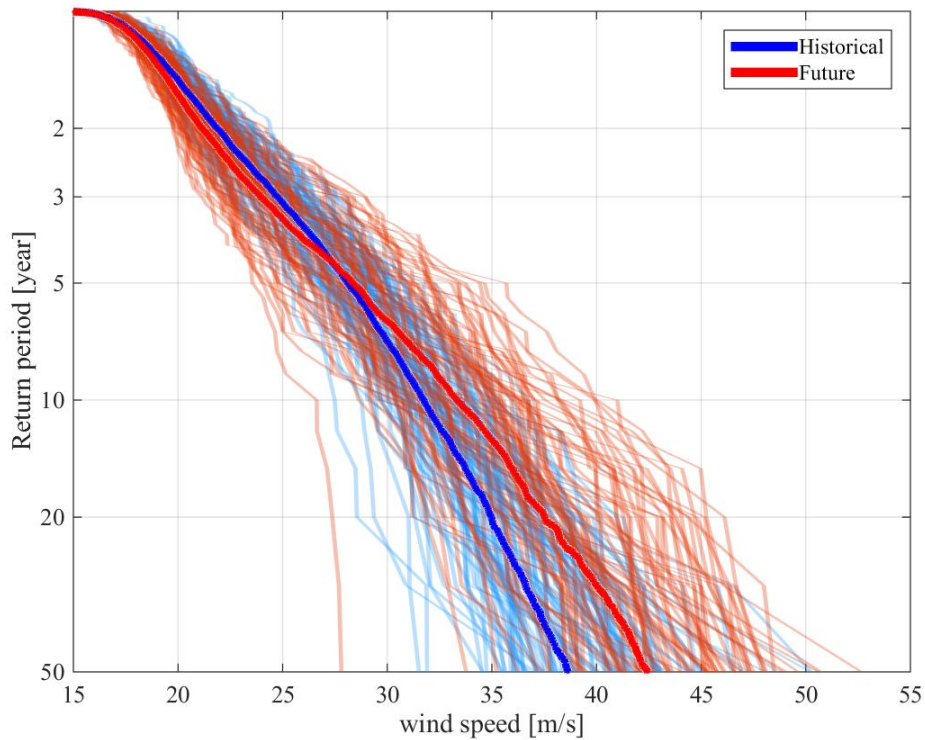


Figure 8. Exceedance probability of U_{10} at the nearest point to the Osaka bay. Thick line is derived from overall ensemble and thin line is each ensemble value.

3.3 Storm surge at the Osaka and Tokyo bay

Table 1. 50 year return value of storm surge deviation at the Osaka bay

Experiment	Overall	Max	Upper 30 %	Lower 30 %	Min
Historical	2.05 m	3.42 m	2.39 m	2.03 m	1.49 m
Future	2.46 m	3.79 m	2.79 m	2.38 m	1.09 m

Table 2. Same as Table 1 but for the Tokyo bay

Experiment	Overall	Max	Upper 30 %	Lower 30 %	Min
Historical	1.27 m	2.02 m	1.45 m	1.29 m	0.96 m
Future	1.49 m	2.43 m	1.66 m	1.43 m	1.00 m

50 years return value of storm surge deviation at the Osaka bay is estimated. The result is shown in Table 1. The value derived from overall ensembles, maximum value in ensembles, upper 30 % value, lower 30 % value and minimum value are shown. The historical value is estimated as 2.05 m and the projected changes is 0.41 m increase. Observed maximum storm surge deviation at the Osaka bay is 2.45m. Projected changes in maximum, upper and lower 30% value show also 0.4 m increases. Projected changes in minimum value indicate 0.4 m decrease, although the minimum value is statistically unstable. In case of 2 year return value, projected change in overall value is 0.06 decrease (Historical value is 0.69 m). These projected decreases in storm surge deviation of shorter return period and increases in extreme storm surge deviation of

longer return period correspond to the tendency of wind speed and also tropical cyclone.

Table 2 is the result of the Tokyo bay. The historical value is estimated as 1.27 m and the projected changes is 0.22 m increase. Same as the Osaka bay, the projected changes in storm surge deviation of shorter and longer return period (below and beyond about 5 years) are positive and negative, respectively.

3.4 Storm surge along global coast

50 year return value of storm surge deviation along global coast roughly correspond to that of wind speed shown in Figure 7. Projected increases in storm surge deviation can be seen in the 15 – 35°N of the Northern Hemisphere. At the East Asia such as China to west of Japan, projected increases in wind speed are about 10 % and those in storm surge deviation are larger than wind speed, over 20 %. On the other hand, decreases in storm surge deviation are projected in the Southern Hemisphere. This is because projected intensification of tropical cyclone is weak and decreases in frequency are remarkable in the Southern Hemisphere.

4. Summary

Long-term assessment of storm surge risk based on the large ensemble climate experiment (d4PDF), 6000 years historical climate experiment and 5400 years future climate experiment under the assumption of 4K global temperature increasing in comparison with the present climate, were conducted. The d4PDF can provide the statistically-stable estimation of extreme event, $O(10)$ to $O(100)$ years return event, for tropical cyclone and storm surge. The main results of this study is below.

- Decreases in tropical cyclone frequency, intensification of extreme tropical cyclone and shift of representative storm track are projected clearly.
- The projected changes in extreme wind speed and storm surge deviation depend on region. The clear increases in 50 year return value of storm surge deviation are projected in the 15 – 35°N latitudes.
- The projected increases in storm surge deviation at the Osaka and Tokyo bay are 0.4m and 0.2m, respectively.

Acknowledgements

This research was supported under the TOGO and SOUSEI Program by the Ministry of Education, Culture, Sports, Science, and Technology (MEXT). The Earth Simulator supercomputer was used in this study as “Strategic Project with Special Support” of JAMSTEC.

References

- Emanuel, K., 2005. Increasing destructiveness of tropical cyclones over the past 30 years, *Nature*, 436: 686–688.
- Fujii T. and Y. Mitsuta, 1986. Synthesis of a stochastic typhoon model and simulation of typhoon winds, *Annuals Disaster Prevention Research Institute, Kyoto University*, 29(B-1): 229-239 (in Japanese).
- Hirahara, S., M. Ishii, and Y. Fukuda, 2014. Centennial-scale sea surface temperature analysis and its uncertainty, *J. Climate*, 27: 57–75.
- IPCC-AR5, 2013. *Climate Change 2013: The Physical Science Basis. Contribution of Working Group I to the Fifth Assessment Report of the Intergovernmental Panel on Climate Change*, Cambridge University Press.
- Kim, S. Y., Yasuda, T., & Mase, H., 2008. Numerical analysis of effects of tidal variations on storm surges and waves, *Applied Ocean Research*, 30(4): 311-322.
- Knapp, K. R., Kruk, M. C., Levinson, D. H., Diamond, H. J., and Neumann, C. J., 2010. The international best track archive for climate stewardship (IBTrACS) unifying tropical cyclone data, *Bulletin of the American Meteorological Society*, 91(3): 363-376.
- Kobayashi, S. and Coauthors, 2015. The JRA-55 Reanalysis: General specifications and basic characteristics. *Journal of the Meteorological Society of Japan*, 93: 5–48.
- Mizuta, R., A. Murata, M. Ishii, H. Shiogama, K. Hibino, N. Mori, O. Arakawa, Y. Imada, K. Yoshida, T. Aoyagi, H. Kawase, M. Mori, Y. Okada, T. Shimura, T. Nagatomo, M. Ikeda, H. Endo, M. Nosaka, M. Arai, C. Takahashi, K. Tanaka, T. Takemi, Y. Tachikawa, K. Temur, Y. Kamae, M. Watanabe, H. Sasaki, A. Kitoh, I. Takayabu, E. Nakakita, and M. Kimoto, 2016. Over 5000 years of ensemble future climate simulations by 60 km global and 20 km regional atmospheric models, *Bulletin of the American Meteorological Society*, doi:10.1175/BAMS-D-16-0099.1.

- Mizuta, R., H. Yoshimura, H. Murakami, M. Matsueda, H. Endo, T. Ose and S. Kusunoki, 2012, Climate simulations using MRI-AGCM3.2 with 20-km grid, *Journal of the Meteorological Society of Japan*, 90A: 233-258.
- Mori, N., 2012, Projection of Future Tropical Cyclone Characteristics based on Statistical Model, In *Cyclones Formation, Triggers and Control*, Nova Science Publishers, Inc: 249-270.
- Murakami, H., 2014, Tropical cyclones in reanalysis data sets. *Geophys. Res. Lett.*, 41: 2133–2141.
- Murata, A., H. Sasaki, M. Hanafusa and K.Kurihara, 2013, Estimation of urban heat island intensity using biases in surface air temperature simulated by a nonhydrostatic regional climate model, *Theoretical and applied climatology*, 112(1-2): 351-361.
- Myers, V. A. and W. Malkin, 1961, Some properties of hurricane wind fields as deduced from trajectories, *US Department of Commerce, Weather Bureau*.
- Nakajo, S., N. Mori, T. Yasuda and H. Mase, 2014, Global stochastic tropical cyclone model based on principal component analysis with cluster analysis, *Journal of Applied Meteorology and Climatology*, 53: 1547-1577.
- Taylor, K. E., R. J. Stouffer, and G. A. Meehl, 2012, An overview of CMIP5 and the experiment design, *Bulletin of the American Meteorological Society*, 93(4): 485–498.
- Woodruff, J. D., J.L. Irish and S.J. Camargo, 2013, Coastal flooding by tropical cyclones and sea-level rise, *Nature*, 504(7478): 44-52.